An Experimental Study of the Flexural Performance of Hybrid Internally Reinforced Concrete Beams with Steel Bars, FRP Bars, Geogrid, and GFRP Mesh

Ban Abd Abbas Khudhair
Department of Civil Engineering, College of Engineering, University of Babylon, Babylon, Iraq
eng936.ban.abad@student.uobabylon.edu.iq (corresponding author)

Hayder Mohammed Al-Khafaji
Department of Civil Engineering, College of Engineering, University of Babylon, Babylon, Iraq
eng.hayder.mj@uobabylon.edu.iq

Received: 7 February 2025 | Revised: 24 February 2025 and 1 March 2025 | Accepted: 7 March 2025

 DOI: https://doi.org/10.48084/etasr.10504

ABSTRACT

This study investigates the flexural performance of Reinforced Concrete (RC) beams internally reinforced with steel bars, Glass Fiber Reinforced Polymer (GFRP) bars, geogrid, and GFRP meshes. The experimental program consists of casting and testing twelve RC beams, including one reference beam without any strengthening and 11 strengthened beams. The key variables examined involve the number and material type of reinforcement mesh layers as well as the number and diameter of GFRP bars. The results indicate that increasing the area of added GFRP bars enhances the ultimate strength by about 37.90% and 20.22% for the beam with two GFRP bars with a diameter of 10 mm and two of 8 mm, respectively, concerning the reference beam. The increase in the area of added GFRP mesh is directly proportional with the beam failure load. The geogrid mesh improved the ultimate strength of the beams slightly more than the GFRP mesh. The addition of reinforcing mesh generally led to an increase in the Ductility Factor (DF) of the beams, but it appeared that the use of geogrid mesh led to an even greater increase. Finally, the mixing of geogrid and GFRP mesh did not significantly affect the DF value.

Keywords-GFRP bars; geogrid mesh;concrete beams; flexural; internal reinforcement; GFRP mesh

I. INTRODUCTION

In recent years, various researchers have improved RC buildings using geogrid, a geosynthetic material known for its exceptional flexibility. The utilization of welded wire mesh as ferrocement laminate has demonstrated many benefits, including remarkable durability, ductility, and toughness. Furthermore, ferrocement may be readily shaped into any form to match the contours of the components requiring repair [1-4]. Glass fiber is predominantly produced from silica sand and is available in various grades within the commercial sector. Glass fiber composites possess excellent thermal and electrical insulation properties. GFRP composites have revolutionized the construction industry by offering innovative and sustainable solutions, and are used in structural elements, such as bars, grids, and profiles. Steel rebars in concrete construction are being substituted by GFRP bars. GFRP is considered resistant to corrosion and to chemical assaults from chloride ions and low pH, and electrically non-conductive. On the other hand, GFRP bars exhibit erratic plastic behavior and diminished ductility, and may display brittleness and susceptibility to cracking or fracturing under sudden impact, while incurring a higher cost compared to steel bars [5, 6].

Authors in [7] evaluated the flexural behavior and serviceability behavior of geopolymer concrete beams strengthened with GFRP bars by a 2-point static load test. The findings indicated that the bar diameter did not significantly affect the bending strength of the samples. The serviceability performance of a beam improves with a higher reinforcement ratio. The mechanical interlock and frictional forces of the sand layer effectively created a strong link between the concrete and the GFRP bars. The predictive equations of ACI-4401.R-06 generally underestimate beam strength. The evaluated beams demonstrated superior bending-moment capacity relative to the previously examined Fiber Reinforced Polymer (FRP) RC beams. In [8], an analysis was performed on six concrete beams reinforced with a combination of GFRP and steel bars. Additionally three concrete beams were fabricated and evaluated using solely steel bars for reinforcement. The flexural behaviors of the examined beams were compared to theoretical models. The results indicated that under the

prescribed service load, the GFRP-steel RC beams displayed a faster increase in crack width and deflection than the steel-RC beams. GFRP-steel RC beams exhibited an ultimate flexural capacity ranging from 91.0% to 97.0% of that of steel-RC beams, while maintaining an equivalent total quantity of GFRP and steel reinforcement.

The bending properties of concrete beams reinforced with GFRP and Carbon Fiber Reinforced Polymer (CFRP) bars were investigated and compared to theoretical results derived from ACI and Eurocode [9]. Twelve RC beams were examined with dimensions of 13 × 22 × 220 cm, augmented with varying diameters of GFRP and CFRP. The reinforcement ratio and concrete strength substantially affected the performance of GFRP, CFRP, and RC beams, having resulted in decreased deflection and crack width aligning closely with the criteria established by ACI. Geogrids are utilized to reinforce asphalt concrete layers, stabilize and restrict soil retaining structures, and alleviate progressive cracking in pavements. Geogrids are categorized into two types: uniaxial and biaxial. Uniaxial geogrids are mostly utilized for retaining walls and the stabilization of steep slopes. Biaxial geogrids are predominantly utilized in highway construction due to their exceptional tensile strength in both horizontal and vertical directions. Fiber and wire mesh are often used interchangeably in concrete components. Fiber mesh is more appropriate for fragile concrete structures and thin concrete layers, while wire mesh is generally utilized for heavier concrete forms [10-12]. Fiberglass mesh exhibits extraordinary durability, superior insulating properties, high tensile strength, remarkable chemical resistance, and can endure extreme temperatures of up to 600 °C without damage. Utilizing this specialized fabric enables the production of glass fiber mesh that exhibits alkali resistance and non-combustibility. As a result, they are/it is ideally suited for various applications, including soil stabilization and concrete building reinforcement [13]. In [14], the effectiveness of Steel Wire Mesh (SWM) and polymer mortars in improving the flexural capacity of concrete beams was investigated. The primary test variables examined were the quantity of longitudinal SWM reinforcements and the load profile. The results demonstrated the feasibility of repairing and improving RC components using SWM materials. In addition, the maximum strength of RC T-beams, enhanced with SWM composites, remained constant irrespective of the load history throughout the reinforcing process. This study aims to develop a design technique capable of accurately predicting the flexural performance of T-beams reinforced with SWM composites. The use of innovative composites to improve concrete beam performance was explored in [15]. The wire mesh epoxy composite was utilized to externally affix one to five layers onto a basic concrete beam. The flexural performance of the beam specimens was assessed among those reinforced with wire mesh layers, those reinforced with carbon fiber, and those reinforced with a combination of wire mesh, epoxy, and carbon fiber composites. The test results demonstrated that the integration of wire mesh through epoxy significantly improved the flexural performance of the concrete samples. Moreover, the additional wire mesh layers significantly strengthened the flexural capacity and energy absorption of the cracking category. Finally, the wire mesh-epoxy composite exhibited enhanced flexural strength and ductility relative to that carbon fiber. The efficacy of Lightweight Concrete (LWC) beams was examined in [16]. Compared to traditional concrete beams, LWC beams exhibited enhanced load-deflection, energy absorption, and ductility performance indices. The integration of internal mesh reinforcement into the LWC beam improved its load-bearing capacity without increasing its bulk or weight. This reinforcement comprised four layers of Welded Wire Mesh (WWM) placed 15 mm apart, followed by four layers spaced 10 mm apart, and finally four layers of mesh alternating between 15 mm and 10 mm. The beam, reinforced with WWM highlighted improved load-bearing capacity and withstood significant deflection without imminent failure. WWM integrates internal reinforcement to manufacture steel rebars, operating as a monolithic structure under load. The internal reinforcement of the structure using WWM enhanced its load-bearing capacity by 25%. This design element results in less strain on tension bars and enhanced load capacity.

Authors in [17] evaluated the influence of different material meshes on the flexural strength of concrete beams to determine the internal reinforcing effect. Eleven RC beams were tested utilizing a four-point bending method. The reinforcement for flexure and shear employed in all 11 beams was consistent. Various quantities of layers and combinations of these chemicals were employed along with geogrid, GFRP, and steel meshes. A solitary beam was fabricated employing a U-shaped mesh for each material. The results revealed that the failure load capabilities of the composite beams exhibited a percentage increase ranging from approximately 3% to 25% in comparison to the control beam. Furthermore, the U-shaped mesh design of the beams indicated a 17% greater load capacity than their straight mesh counterparts. The ductility ratio showed a substantial increase of approximately 82% to 136% when the layer count escalated from 1 to 3.

The current investigation focuses on determining how the number and material type of reinforcement mesh layers, and the number and material type of reinforcement bar layers affected the results.

II. EXPERIMENTAL PROGRAM

The experimental program consists of casting and testing 12 RC beams, including 1 reference beam without any strengthening and 11 strengthened beams.

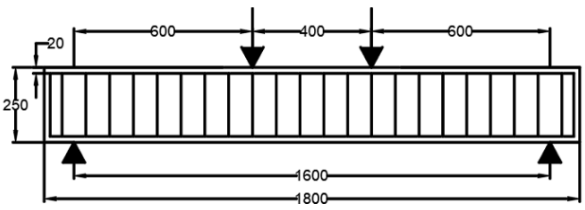

Fig. 1. Details of the tested beams.

The key variables investigated in this study involve the number and material composition of the reinforcement mesh layers as well as the quantity and diameter of the GFRP bars. All beams have the same length, width, height, and steel

reinforcement, and were subjected to dual point loads, as illustrated in Figure 1. The reinforcement details are presented in Figures 1 and 2, while Table I outlines the configurations of the test beams.

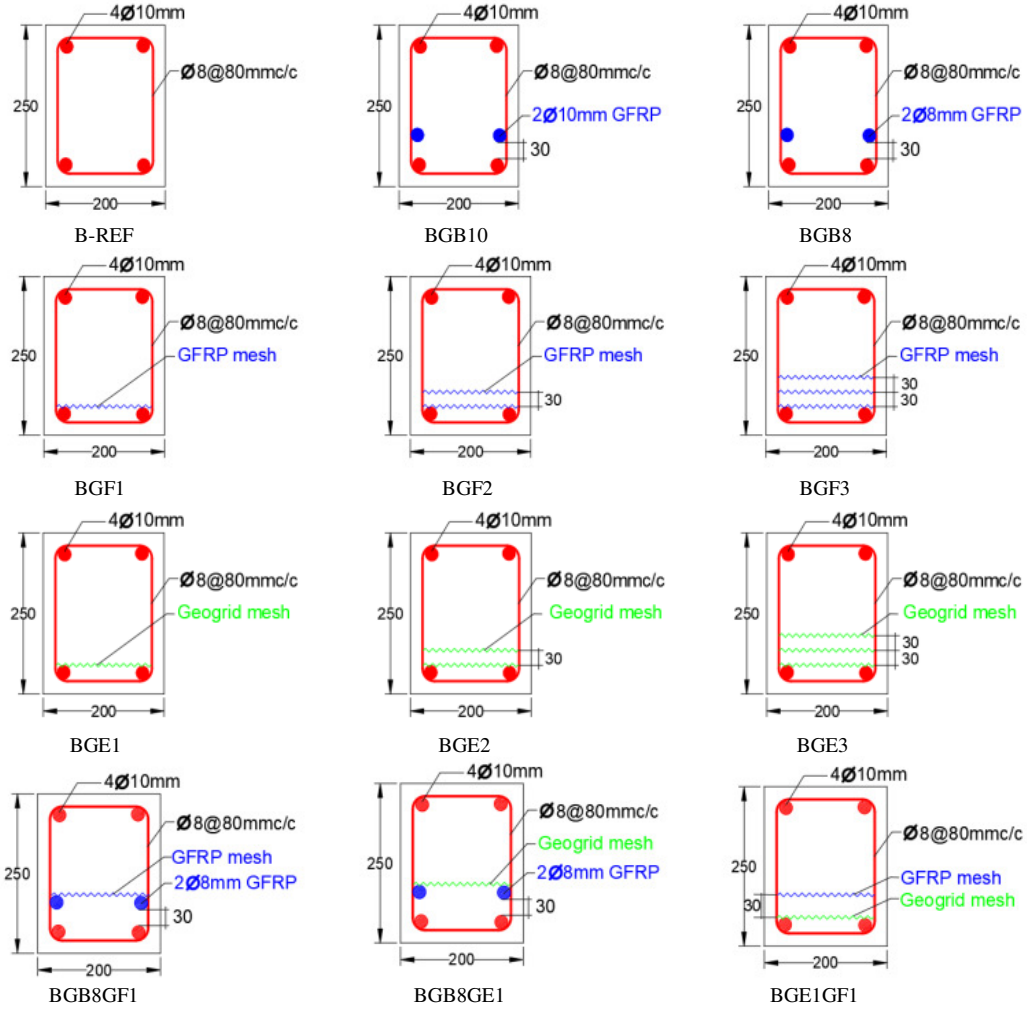

Fig. 2. Cross section of the tested beams.

TABLE I. TESTED BEAM DETAILS

Beam ID	Diameter of GFRP bars (mm)	Type of mesh layer	Number of mesh layers
B-REF	-	-	-
BGB10	10	-	-
BGB8	8	-	-
BGF1	-	GFRP	1
BGF2	-	GFRP	2
BGF3	-	GFRP	3
BGE1	-	Geogrid	1
BGE2	-	Geogrid	2
BGE3	-	Geogrid	3
BGB8GF1	8	GFRP	1
BGB8GE1	8	Geogrid	1
BGE1GF1	-	Geogrid+GFRP	1+1

TABLE II. TENSILE CHARACTERISTICS OF STEEL REINFORCING REBARS

Nominal diameter (mm)	Area (mm^2)	Average yield tensile stress (Mpa)	Average ultimate tensile strength (Mpa)	Elongation in ultimate stress (%)
8	50.3	501	593	11.00
10	78.5	560	662	11.64

Table II illustrates the tensile characteristics of the steel reinforcing bars in accordance with the ASTM A615. The steel bars were examined in the Babil Tower in order to conduct studies and scientific research on their properties and performance.

Table VI shows the details of the mix proportion of concrete, taken from [18].

TABLE III. MECHANICAL PROPERTIES OF GFRP BARS

Property	GFRP bar 8 mm	GFRP bar 10 mm
Ultimate tensile strength (MPa)	1080	980
E- modulus (GPa)	≥40	≥40
Cross section area (mm^2)	50	73
Diameter (mm)	8	10
Density (g/cm^3)	2.2	2.2

TABLE IV. PROPERTIES OF GEOGRID MESH

Properties		Unit	100/100
Tensile strength	MD CMD	kN/m (Min.)	100 100
Elongation at maximum load	MD CMD	% (±%2)	12
Elongation at nominal load	MD CMD	% (±%2)	10
Mesh size	MD CMD	mm (±3)	30 26
Roll width	MD CMD	m (±%1.5)	5.25 6
Roll length	MD CMD	m (±%1.5)	50
MD = Machine Direction, CMD = Cross Machine Direction			

TABLE V. PROPERTIES OF FIBERGLASS MESH

Product name	Fiberglass mesh	
Specification	5 x 5 mm	
Weight	160 g ± 5 g/m^2	
Roll length	50 m	
Roll width	1 m	
Thread tex	Wrap	100
	Weft	450
Tensile strength (N/5 cm)	Wrap	1100
	Weft	850

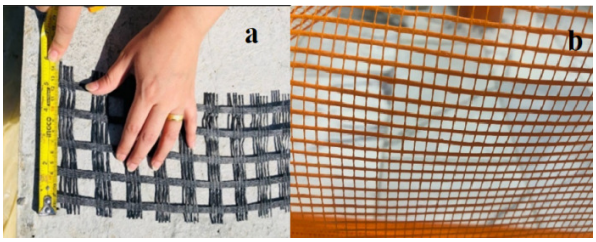

Fig. 3. (a) Geogrid mesh and (b) fiberglass mesh.

TABLE VI. DETAILS OF MIX PROPORTION MATERIALS

Cement (kg/m^3)	Fine agg. (kg/m^3)	Coarse agg. (kg/m^3)	W/C ratio
400	700	1056	0.52

III. EXPERIMENTAL RESUTLS

A. Hardened Concrete Properties

The cube compression test was conducted in accordance with BS 1881: Part 116, the cylinder compression test was carried out according to ASTM C 39M-17, the splitting tensile strength was measured according to ASTM C 496/C496M, and the test of modulus of rupture was conducted according to ASTM C78.

Fig. 4. Installation of reinforcement, and mesh and concrete pouring.

TABLE VII. HARDENED CONCRETE PROPERTY RESULTS

Cube compressive strength (MPa)	Cylinders compressive strength (MPa)	Splitting tensile strength (MPa)	Modulus of rupture (MPa)
39.8	32.6	3.46	3.91

B. Initial Crack Loads

Table VIII presents the experimental findings related to cracking loads, deflections, and failure loads. The initial crack was observed at an applied load between 20 and 28 kN with the First Crack Load (Pcr) to Ultimate Load (Pu) percentage ranging from 18.38% to 26.56%. This suggests that the addition of GFRP bars resulted in a decrease in the Pcr to Pu ratio, while the incorporation of GFRP or Geogrid mesh led to an increase in the same ratio.

TABLE VIII. ULTIMATE AND CRACKING LOADS

Beam ID	Pcr (kN)	Pu (kN)	Pcr/Pu (%)
B-REF	20	87.10	22.96
BGB10	25	120.11	20.81
BGB8	20	104.71	19.1
BGF1	25	94.11	26.56
BGF2	25	97.25	25.71
BGF3	25	99.31	25.17
BGE1	25	97.21	25.72
BGE2	25	103.77	24.09
BGE3	25	106.59	23.45
BGB8GF1	20	108.81	18.38
BGB8GE1	28	112.03	24.99
BGE1GF1	25	97.98	25.52

C. Deformability of the Examined Beams under the Imposed Load

Deformability pertains to the strain within a body, the curvature of a section, the tilt of a member, and the deflection of a member. The chosen serviceability limit was the experimental Pu divided by 1.7, as proposed in [19], due to the absence of undesired breaking or deformation at this threshold.

Consequently, Table IX contains the relevant mid-span deflections for the service load, Pu of the reference beam group, and ultimate applied load for all beams. The selected Pu of the reference beam (87.1 kN) within the group is crucial for comparing deflections under a constant load, which serves as a marker of beam stiffness.

TABLE IX. MID SPAN DEFLECTION AT DIFFERENT LOADING STAGES

Beam ID	Service Deflection (mm)	At 87.1 kN		Ultimate Deflection (mm)	P_{ult} (kN)
		Deflection (mm)	Deflection Decrease Percentage (%)		
B-REF	4.31	20.52	Ref.	20.52	87.10
BGB10	3.75	6.10	70.3	26.81	120.11
BGB8	4.60	10.87	47.0	25.51	104.71
BGF1	3.95	12.05	41.2	22.62	94.11
BGF2	3.56	6.60	67.8	22.14	97.25
BGF3	3.42	6.20	69.8	23.24	99.31
BGE1	3.89	13.40	34.7	26.11	97.21
BGE2	3.87	7.90	61.5	27.39	103.77
BGE3	3.86	6.50	68.3	28.63	106.59
BGB8GF1	4.44	8.50	58.6	27.22	108.81
BGB8GE1	4.90	9.77	52.4	30.33	112.03
BGE1GF1	4.75	14.40	29.8	26.12	97.98

As per the ACI-318M-19 [20] guidelines, the maximum allowable deflection for flat roofs not supporting or affixed to non-structural components, and susceptible to damage from significant deflections is L/180, which is roughly 8.89 mm. Table VII indicates that all examined beams remained below this limit under service load conditions. Figures 5-9 display that all tested beams initially exhibited linear deflection. However, subsequent to the cracking load, they exhibited semi-linear deflection with an increasing load. The slope of the deflection lines, though, was significantly reduced compared to the pre-cracking phase with the deflection curves diverged according to the extent of cracking and the degree of stiffness degradation. Additionally, the angle of this linear segment differed among samples. As loads approached the Pu, tested beam deflection curves diverged from the control beam's deflection curve. At the Pu of the reference beam, for all strengthened beams, the mid-span deflection decreased concerning the reference beam. This is an indication of increased stiffness, where the beam of the two GFRP bars of 10 mm without any mesh decreased by 70.3%. The beam with one layer of GFRP mesh and one layer of geogrid mesh decreased by 29.8% concerning the reference beam.

1) GFRP Bars Addition Effect

The effect of adding GFRP bars on the load against the mid-span deflection relationship is illustrated in Figure 5.

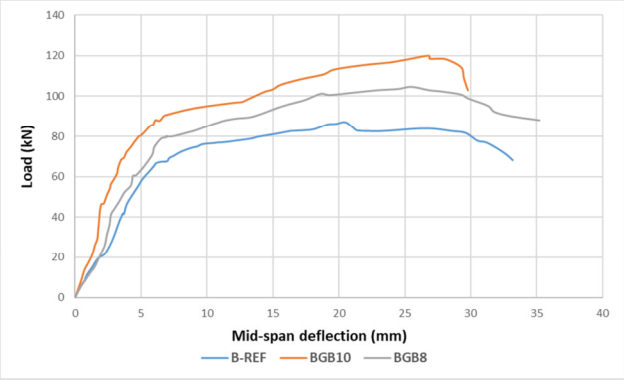

Fig. 5. GFRP bar effect on load-deflection curves.

It is demonstrated that the three beams exhibited identical stiffness in the region of elasticity. However, post-cracking of the concrete, the augmentation of the GFRP bar area was proportional to beam stiffness.

2) Mesh Layer Number Addition Effect

Figure 6 depicts the GFRP mesh layer number addition effect on mid-span deflection relationship.

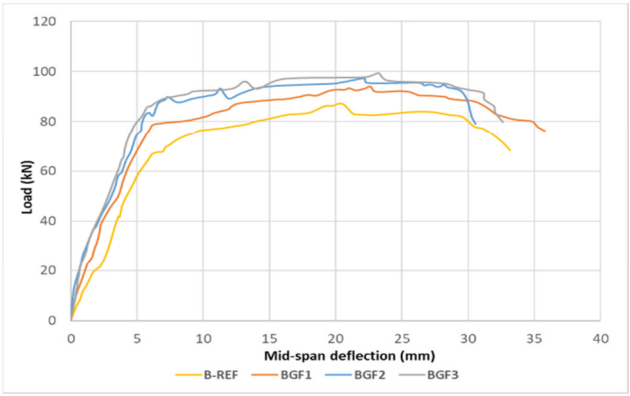

Fig. 6. GFRP mesh layer number effect on load-deflection curves.

In Figure 7, the impact of the added geogrid mesh layer number on the load against mid-span deflection relationship can be observed. The load-deflection curves indicate that the four beams exhibit identical stiffness in the region of elasticity. However, post-cracking of the concrete, an increase in the quantity of GFRP or geogrid mesh correlates directly with beam stiffness.

3) Mesh Material Addition Effect

Figure 8 portrays the impact of the added mesh material on the load against mid-span deflection relationship. From the load-deflection curves, it is evident that the effect of GFRP mesh is almost similar to the geogrid mesh but the mixing of GFRP and geogrid mesh decreases the stiffness of the beam.

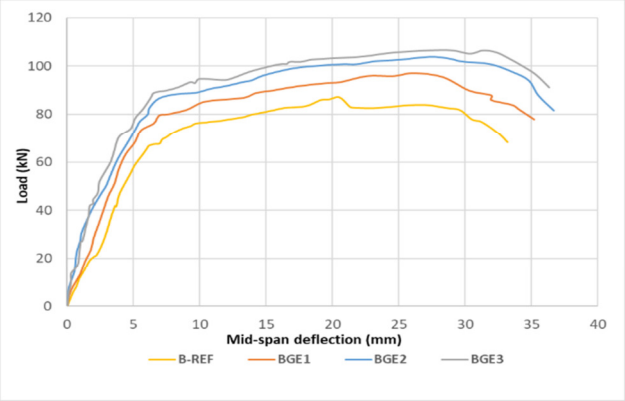

Fig. 7. Geogrid mesh layer number effect on load-deflection curves.

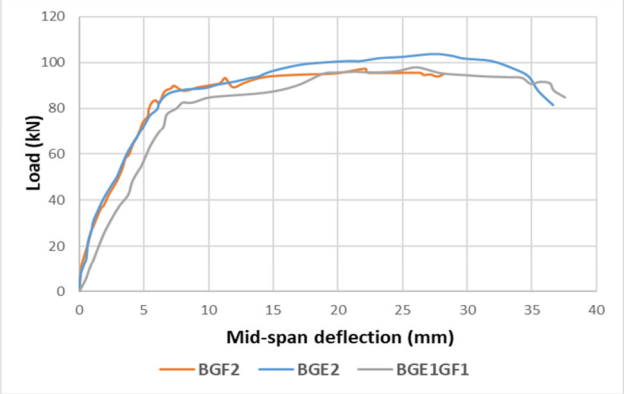

Fig. 8. Geogrid and GFRP mesh mixing effect on load-deflection curves.

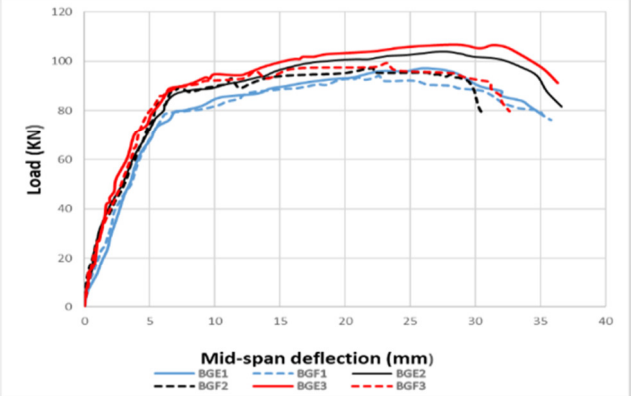

Fig. 9. Mesh material addition effect.

Figure 9 shows the impact of the added mesh material type on the load against mid-span deflection relationship. It is observed that the addition of the geogrid mesh slightly increases the failure load value and greatly increases the corresponding deflection value, suggesting a slight increase in the beam's overall stiffness while also greatly enhancing its ductility. This indicates that the addition of the geogrid mesh enhances the structural performance of the beam, providing a beneficial balance between the load-bearing capacity and deformation tolerance.

D. Load-Carrying Capacity and Failure Mode

Only flexural cracks developed in all beams. When the applied load caused serious flexural stresses in the middle part of the span, nearly vertical flexural cracks were formed in the extreme tensile fibers of the bottom section, nearby the maximum bending moment section. By increasing the level of loading, the number of vertical flexural cracks grew substantially, their length increased, their ends took a more horizontal route, and the flexural cracks tended to flatten. The aforementioned inclined cracks proceeded as a result of the application of the load, whereas the region over which the crack seemed to extend and the direction of these cracks oriented toward the points of the applied force. All beams failed due to fractures originating from the beam soffit at the maximum bending moment. These cracks propagated toward the upper zone due to steel yielding, culminating in compression failure near the mid-span's top.

Table X presents the Pu for all the tested beams in comparison with the failure load value of the reference beam. The maximum value is observed for BGB10 beam with a Pu of 120.11 kN, suggesting an increase of 37.90%, and the minimum for BGF1 beam with Pu of 94.11 kN, indicating an increase of 8.00%. All strengthened beams presented in Table X have a Pu higher than the reference one.

TABLE X. ULTIMATE LOADS FOR ALL BEAMS

Beam ID	Pu (kN)	Increase percentage in Pu (%)
B-REF	87.10	Ref.
BGB10	120.11	37.90
BGB8	104.71	20.22
BGF1	94.11	8.00
BGF2	97.25	11.65
BGF3	99.31	14.00
BGE1	97.21	11.61
BGE2	103.77	19.14
BGE3	106.59	22.38
BGB8GF1	108.81	24.90
BGB8GE1	112.03	28.60
BGE1GF1	97.98	12.50

1) Glass Fiber Reinforced Polymer Bar Addition Effect on Pu

Table IX displays that the increase of the area of added GFRP bars results in an ultimate strength enhancement by about 37.9% and 20.22% for the beam with two GFRP bars of 10 mm diameter and the beam with two GFRP bars of 8 mm diameter, respectively, concerning the reference beam.

2) Mesh Layer Number Addition Effect on Pu

Table IX demonstrates that increasing the area of added GFRP mesh results in an enhancement of ultimate strength by about 8%, 11.65%, and 14% for the beams with one, two, and three GFRP mesh layers, respectively, concerning the reference beam. Additionally, increasing the area of added geogrid mesh results in an enhancement of the ultimate strength by about 11.61%, 19.14%, and 22.38% for the beams with one, two, and three geogrid mesh layers, respectively, concerning the reference beam. The geogrid mesh improved the ultimate strength of the beams slightly more than the GFRP mesh.

Fig. 10. Final crack pattern of specimens: (a) B-REF, (b) BGB10, (c) BGB8, (d) BGF1, (e) BGF2, (f) BGF3, (g) BGE1, (h) BGE2, (i) BGE3, (j) BGB8GF1, (k) BGB8GE1, and (l) BGE1GF1.

3) Mesh Material Addition Effect on Pu

Table XI shows that the geogrid mesh slightly increases the Pu value, while the mixing of GFRP and geogrid mesh does not affect the Pu.

TABLE XI. MIXING EFFECT OF ADDED MESH MATERIAL ON ULTIMATE LOAD

Beam ID	Pu (kN)	Increase percentage in Pu (%)
BGF2	97.25	Ref.
BGE2	103.77	6.70
BGE1GF1	97.98	0.75

According to Table XII, the geogrid mesh slightly increases the failure load value, where replacing the GFRP mesh with geogrid mesh leads to a small enhancement in the ultimate strength around 3.30%, 6.70%, and 7.33% for the beams with one, two, and three mesh layers, respectively.

TABLE XII. MESH MATERIAL ADDITION EFFECT ON ULTIMATE LOAD

Beam ID	Pu (kN)	Increase percentage in Pu (%)
BGF1	94.11	Ref.
BGE1	97.21	3.3
BGF2	97.25	Ref.
BGE2	103.77	6.7
BGF3	99.31	Ref.
BGE3	106.59	7.33

E. Ductility Index

The ductility index quantifies a structural member's ability to endure significant deformations. The ratio of mid-span deflection at failure loads over/to mid-span deflection at the first yielding of tensile main rebars. The DF for each specimen is presented in Table XIII and defined as the ratio of ultimate deflection and/to the yield deflection. The addition of GFRP bars, in addition to the existing reinforcement steel, resulted in a significant increase in the DF. The addition of reinforcing mesh generally led to an increase in the beams' DF, but it appeared that the use of geogrid mesh led to a greater increase than GFRP mesh utilization. The mixing of geogrid and GFRP mesh did not significantly affect the ductility coefficient value.

TABLE XIII. DF OF ALL BEAMS

Beam ID	Yeilding deflection (mm)	Ultimate deflection (mm)	DF	Increase percentage in DF (%)
B-REF	8.40	20.52	2.44	Ref.
BGB10	6.81	26.81	3.94	61.4
BGB8	6.20	25.51	4.11	68.4
BGF1	7.26	22.62	3.10	27.0
BGF2	5.90	22.14	3.75	53.7
BGF3	6.02	23.24	3.86	58.2
BGE1	7.50	26.11	3.48	42.6
BGE2	6.40	27.39	4.28	75.4
BGE3	6.30	28.63	4.54	86.1
BGB8GF1	5.90	27.22	4.61	88.9
BGB8GE1	6.10	30.33	4.97	103.7
BGE1GF1	8.50	26.12	3.07	25.8

IV. CONCLUSION

This study investigated the flexural behavior of Reinforced Concrete (RC) beams with various internal reinforcement configurations including steel bars, Fiber Reinforced Polymer (FRP) bars, and Glass Fiber Reinforced Polymer (GFRP) geogrid meshes. The research objective was to assess how the quantity and material composition of the reinforcement mesh layers and bar layers affected the results .

The initial crack was observed at an applied load of 20 kN to 28 kN, with a variation in the First Crack Load (Pcr) to Ultimate Load (Pu) percentage ranging from 18.38% to 26.56%. The addition of GFRP bars resulted in a decrease in the Pcr/Pu percentage. In contrast, the addition of GFRP or geogrid mesh led to an increased Pcr/Pu percentage.

At the Pu of the reference beam (87.1 kN), all strengthened beams exhibit a reduction in mid-span deflection compared to the reference beam, indicating enhanced stiffness. The beam reinforced with two 10 mm GFRP bars, without any mesh, shows a decrease of 70.3%, while the beam with one layer of GFRP mesh and one layer of geogrid mesh demonstrates a decrease of 29.8% relative to the reference beam. All beams failed due to cracks appearing from the underside of the beams at the point of maximum bending stress. These cracks then moved upwards as a result of the steel reinforcement yielding, ultimately leading to compressive failure in the upper region at mid-span.

Increasing the area of the included GFRP bars resulted in an enhancement of ultimate strength by 37.9% and 20.22% for the beam with two GFRP bars of 10 mm diameter and the beam with two GFRP bars of 8 mm diameter, respectively, compared to the reference beam. These findings align with [21]. Furthermore, the addition of the GFRP mesh area improved the ultimate strength at 8%, 11.65%, and 14% for the beams with one, two, and three GFRP mesh layers, respectively, supporting prior research findings [22]. Finally, expanding the area of the included geogrid mesh enhanced the ultimate strength at a 11.61%, 19.14%, and 22.38% level for the beams with one, two, and three geogrid mesh layers, respectively. The expansion of the new geogrid mesh area is directly proportional to the beam failure load. The geogrid mesh exhibited a slightly greater enhancement of the beam ultimate strength compared to the GFRP mesh, corroborating with results from [23].

The incorporation of reinforcing mesh frequently enhanced the Ductility Factor (DF) of the beams. However, the use of geogrid mesh produced a more significant improvement relative to the GFRP mesh. Finally, the combination of geogrid and GFRP mesh did not substantially influence the DF value.

REFERENCES

[1] K. Zhang and Q. Sun, "The use of Wire Mesh-Polyurethane Cement (WM-PUC) composite to strengthen RC T-beams under flexure," *Journal of Building Engineering*, vol. 15, pp. 122–136, Jan. 2018, https://doi.org/10.1016/j.jobe.2017.11.008.

[2] M. Mebrahtom *et al.*, "Comparative study of eco-friendly wire mesh configurations to enhance sustainability in reinforced concrete structures," *Scientific Reports*, vol. 14, no. 1, Apr. 2024, Art. no. 8818, https://doi.org/10.1038/s41598-024-59050-2.

[3] B. F. Abdulkareem, A. F. Izzet, and N. Oukaili, "Post-Fire Behavior of Non-Prismatic Beams with Multiple Rectangular Openings Monotonically Loaded," *Engineering, Technology & Applied Science Research*, vol. 11, no. 6, pp. 7763–7769, Dec. 2021, https://doi.org/10.48084/etasr.4488.

[4] B. S. Al-Shathr, H. A. Abdulhameed, and M. M. Mahdi, "Effect of Wire-Mesh Type on Strengthening Reinforced Concrete Beams," *Engineering and Technology Journal*, vol. 40, no. 5, pp. 759–768, May 2022, https://doi.org/10.30684/etj.2021.131159.1009.

[5] *Guide for the Design and Construction of Externally Bonded FRP Systems for Strengthening of Concrete Structures*, ACI Committee 440-2R., American Concrete Institute, MI, USA, 2015.

[6] M. F. K. AlShamaa, M. G. Ghaddar, M. M. Jebur, A. Al-Rumaithi, A. J. Hussain Alshimmeri, and M. Karkush, "Evaluating the Structural Integrity of Cellular Steel Beams with Web Enhancements," in *IOP Conference Series: Earth and Environmental Science*, Karbala, Iraq, Dec. 2024, vol. 1374, Art. no. 012088, https://doi.org/10.1088/1755-1315/1374/1/012088.

[7] G. B. Maranan, A. C. Manalo, B. Benmokrane, W. Karunasena, and P. Mendis, "Evaluation of the flexural strength and serviceability of geopolymer concrete beams reinforced with glass-fibre-reinforced polymer (GFRP) bars," *Engineering Structures*, vol. 101, pp. 529–541, Oct. 2015, https://doi.org/10.1016/j.engstruct.2015.08.003.

[8] X. Ruan, C. Lu, K. Xu, G. Xuan, and M. Ni, "Flexural behavior and serviceability of concrete beams hybrid-reinforced with GFRP bars and steel bars," *Composite Structures*, vol. 235, Mar. 2020, Art. no. 111772, https://doi.org/10.1016/j.compstruct.2019.111772.

[9] N. Kabashi, B. Avdyli, E. Krasniqi, and A. Këpuska, "Comparative Approach to Flexural Behavior of Reinforced Beams with GFRP, CFRP, and Steel Bars," *Civil Engineering Journal*, vol. 6, no. 1, pp. 50–59, Jan. 2020, https://doi.org/10.28991/cej-2020-03091452.

[10] A. Daou, G. Chehab, G. Saad, and B. Hamad, "Experimental and numerical investigations of reinforced concrete columns confined internally with biaxial geogrids," *Construction and Building Materials*, vol. 263, Dec. 2020, Art. no. 120115, https://doi.org/10.1016/j.conbuildmat.2020.120115.

[11] M. S. Eisa, M. E. Basiouny, and E. A. Fahmy, "Drying shrinkage and thermal expansion of metakaolin-based geopolymer concrete pavement reinforced with biaxial geogrid," *Case Studies in Construction Materials*, vol. 17, Dec. 2022, Art. no. e01415, https://doi.org/10.1016/j.cscm.2022.e01415.

[12] M. S. Moawad and A. M. El-Hanafy, "Investigation of the effect of using geogrid, short glass, and steel fiber on the flexural failure of concrete beams," *Alexandria Engineering Journal*, vol. 68, pp. 479–489, Apr. 2023, https://doi.org/10.1016/j.aej.2023.01.054.

[13] R. Krzywoń and S. Dawczyński, "Strength Parameters of Foamed Geopolymer Reinforced with GFRP Mesh," *Materials*, vol. 14, no. 3, Jan. 2021, Art. no. 689, https://doi.org/10.3390/ma14030689.

[14] G. Xing, T. Wu, B. Liu, H. Huang, and S. Gu, "Experimental Investigation of Reinforced Concrete T-Beams Strengthened with Steel Wire Mesh Embedded in Polymer Mortar Overlay," *Advances in Structural Engineering*, vol. 13, no. 1, pp. 69–79, Feb. 2010, https://doi.org/10.1260/1369-4332.13.1.69.

[15] I. M. I. Qeshta, P. Shafigh, M. Z. Jumaat, A. I. Abdulla, Z. Ibrahim, and U. J. Alengaram, "The use of wire mesh–epoxy composite for enhancing the flexural performance of concrete beams," *Materials & Design*, vol. 60, pp. 250–259, Aug. 2014, https://doi.org/10.1016/j.matdes.2014.03.075.

[16] P. Chandramouli, D. Muthukrishnan, V. Sridhar, V. S. Kumar, G. Murali, and N. I. Vatin, "Flexural Behaviour of Lightweight Reinforced Concrete Beams Internally Reinforced with Welded Wire Mesh," *Buildings*, vol. 12, no. 9, Sep. 2022, Art. no. 1374, https://doi.org/10.3390/buildings12091374.

[17] A. K. Hanan, M. D. Muttashar, S. R. Abid, A. M. Yosri, F. Alsharari, and A. farouk Deifalla, "Flexural performance of concrete beams internally reinforced with steel, geogrid and GFRP meshes," *Journal of Materials Research and Technology*, vol. 24, pp. 9156–9170, May 2023, https://doi.org/10.1016/j.jmrt.2023.05.146.

[18] S. R. Jasim and H. M. J. AL-Khafaji, "Improve the Flexural Behavior of One-Way Ribbed Slab by Using CFRP Sheet," *Tikrit Journal of Engineering Sciences*, vol. 31, no. 2, pp. 272–280, Jun. 2024, https://doi.org/10.25130/tjes.31.2.25.

[19] M. A. Mansur, L. M. Huang, K. H. Tan, and S. L. Lee, "Deflections of Reinforced Concrete Beams With Web Openings," *Structural Journal*, vol. 89, no. 4, pp. 391–397, Jan. 1992, https://doi.org/10.14359/3019.

[20] *Building code requirements for structural concrete*, ACI 318M-19, American Concrete Institute, MI, USA, 2019.

[21] X. Ruan, C. Lu, K. Xu, G. Xuan, and M. Ni, "Flexural behavior and serviceability of concrete beams hybrid-reinforced with GFRP bars and steel bars," *Composite Structures*, vol. 235, Mar. 2020, Art. no. 111772, https://doi.org/10.1016/j.compstruct.2019.111772.

[22] M. A. Wafa and K. Fukuzawa, "Characteristics of ferrocement thin composite elements using various reinforcement meshes in flexure," *Journal of Reinforced Plastics and Composites*, vol. 29, no. 23, pp. 3530–3539, Sep. 2010, https://doi.org/10.1177/0731684410377814.

[23] S. Sivakamasundari, A. J. Daniel, and A. Kumar, "Study on Flexural Behavior of Steel Fiber RC Beams Confined With Biaxial Geo-Grid," *Procedia Engineering*, vol. 173, pp. 1431–1438, Jan. 2017, https://doi.org/10.1016/j.proeng.2016.12.206.